Available online at www.sciencedirect.com

SCIENCE DIRECT®

Earth and Planetary Science Letters 227 (2004) 473–480

EPSL

www.elsevier.com/locate/epsl

Dual porosity mechanism for transient groundwater and gas anomalies induced by external forcing

Éric Pili*, Frédéric Perrier[1], Patrick Richon[2]

Commissariat à l'Énergie Atomique, Département Analyse Surveillance Environnement, BP12, 91680, Bruyères-le-Châtel, France

Received 5 January 2004; received in revised form 5 June 2004; accepted 21 July 2004
Available online 5 October 2004
Editor: V. Courtillot

Abstract

The geochemical response of groundwater to external forcing is studied in a tunnel hosted in fractured gneiss near and above an artificial lake having large water level variations. Dripping waters have been monitored in two zones characterized by highly different flow rates representing different contributions of water from matrix porosity and fractures. Transient increases of sulfate and magnesium concentrations, observed in both zones, are not related to meteorology but associated with radon bursts into the tunnel air. This indicates that transient enhancement of conductance, with discharges of saline water and radon from the matrix porosity to the fractures, is a mechanism able to produce both groundwater and gas anomalies, in response to hydrogeological or mechanical processes such as increases in pore pressure or changes in crack geometry. Besides its applications to environmental issues, the proposed discharge mechanism may be relevant for the understanding of geochemical precursors of earthquakes, as an alternative to aquifer mixing.

Keywords: groundwater; major elements, gas; transient anomaly; porosity; fractures

1. Introduction

For theoretical as for practical reasons such as waste disposal or contaminant hydrology, a better knowledge of fractured porous media is required. In particular, the dynamics of fractured porous media in response to external forcing such as meteorology, deformation, or hydrogeological disturbances remains poorly known. To increase our understanding of such systems and to build reliable predictive models, there is a strong need to obtain hydrologic and chemical data from complex but well characterized natural observatories at scales varying from 10 m to 1 km [1]. Our contribution aims at characterizing transient phenomena in a system which is highly dynamical in its water budget as well as in the space and time

* Corresponding author. Tel.: +33 1 69 26 50 11; fax: +33 1 69 26 70 65.
E-mail addresses: Eric.Pili@cea.fr (É. Pili), Frederic.Perrier@cea.fr (F. Perrier), Patrick.Richon@cea.fr (P. Richon).
[1] Tel.: +33 1 69 26 62 79; fax: 33 1 69 26 70 65.
[2] Tel.: +33 1 69 26 52 95; fax: +33 1 69 26 70 65.

0012-821X/$ - see front matter © 2004 Elsevier B.V. All rights reserved.
doi:10.1016/j.epsl.2004.07.043

scales accessible to observation (high flow rates, short transit time, and high return rates for anomalies). For this purpose, we set up a monitoring experiment in a tunnel where drippings give access to groundwater flowing from over 50 m of fractured gneiss. This tunnel is located close to and above the artificial Roselend lake (French Alps) where large seasonal variations in water level induce, in particular, known and reproducible deformation [2]. This mountainous area is also characterized by contrasted precipitation regimes with alternating snow, rain, and dry periods. Major elements in waters were analyzed because of their robustness, sampling and analytical simplicity and their sensitivity to host rock chemistry and mineralogy. In order to get water samples representative of different contributions of matrix porosity and fractures, we compared two zones with different settings (structures and flow rates) and looked for changes in major element concentrations in groundwater over one year. In addition, we monitored the activity of radon-222 in the atmosphere of the tunnel.

2. Geological setting

The Roselend lake, in the French Alps, is a 0.187 km^3 artificial reservoir with yearly water level variations of ca. 70 m (114 m in 1999, the year of this study with the last 10-year emptying of the lake occurring in February–March). The horizontal tunnel, at an altitude of 1576 m, is located less than 150 m west from the west shore of the lake and 19 m above the lake at its highest water level. More on the geographical setting of the area can be found in [2]. This instrumented dead-end tunnel [3] is 128 m long and 2 m in diameter, and had been abandoned for about 30 years. It is entirely hosted in gneiss and capped with gneiss of increasing thickness from 7 m at the entrance to 55 m at its closed end (Fig. 1). At the topographic surface above the tunnel, the soil layer has a thickness of less than 10 cm, as expected in such gneissic, high-range and steep mountainous area. Right above the section studied in the tunnel lies, a dirt road built on no more than 1 m of compacted gneiss blocks, gravel and sands, as determined from

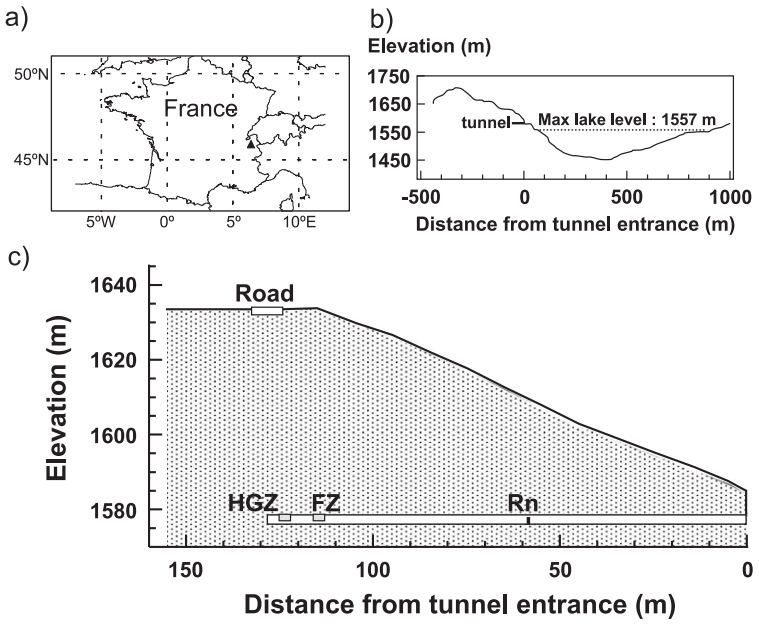

Fig. 1. (a) Location of the Roselend area in France (triangle). (b) Cross-section of the Roselend lake area along N 130°E, adapted from [2], perpendicular to the shore of the lake at the tunnel entrance, showing the local topography, the location of the tunnel, and the maximum level of the lake. The direction of the tunnel is N 65°E from end to entrance. The length of the tunnel is a projection. (c) Cross-section of the Roselend tunnel along its axis showing the location of the two experimental zones (HGZ and FZ) where dripping waters are collected, and the area where radon activity is measured in the air of the tunnel (Rn).

seven drill holes (Fig. 1). The main geological structures observed in the tunnel are steeply dipping and range from foliation (mm-scale), cleavage (dm-scale), quartz veins (cm-to m-scale), fractures and brittle to ductile shear zones (m-to tens of m-scale). Many quartz veins contain accessory chlorite, calcite, and pyrite. Pyrite is also heterogeneously distributed in the host gneiss (quartz, Ca–Na feldspar, biotite, chlorite). The average air temperature in the tunnel is 6.7 °C, with yearly variations smaller than 0.1 °C, and the relative humidity is nearly 100%. Water drips from the roof of the tunnel with droplets leaving a carbonate precipitate.

3. Sampling and analyses

Two zones, 6 m apart, were selected within a distance of 3 to 15 m from the closed end of the tunnel (Fig. 1). In the host gneiss zone (HGZ) the dripping water flow rates are low (~1 ml/h per m^2). In contrast, the highly fractured zone (FZ), partly cemented by a 10-cm-wide quartz vein, has a significantly higher flow rate (~100 ml/h per m^2). Both zones have been equipped with a 2×3-m^2 polymer sheet hung near the roof in such a way that dripping water can be collected at one point by an automated sampler every 4 days. The samplers are serviced every 96 days. The flow rates of water coming out of the polymer sheets have been manually measured at each visit, with an uncertainty better than ±10%. Minor precipitation of calcium carbonate has been observed in the sampling device. Water flow rates at these zones were manually measured four times per year. For reference, other characteristic waters of the Roselend site (dripping waters elsewhere in the tunnel, nearby springs, lake waters, rain and snow) have also been sampled and analyzed. The major cations and anions of the water

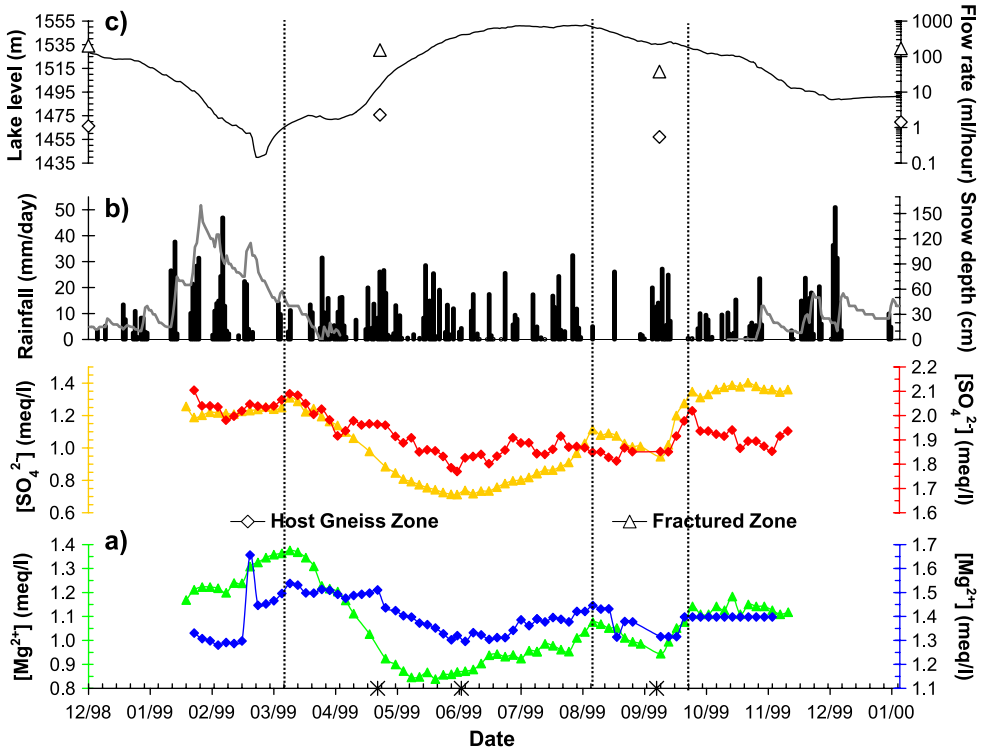

Fig. 2. (a) Tunnel dripping water concentrations in SO_4^{2-} and Mg^{2+} as a function of time in the HGZ (diamonds) and the FZ (triangles). Sampling campaigns within crosses. Dashed lines indicate three main transient increases in concentrations. FZ dripping waters from 07/29/1999 to 12/02/1999 are analyzed by ion chromatography (SO_4^{2-}) and ICP-OES (Mg^{2+}), otherwise by capillary electrophoresis. (b) Rainfall intensity and snow depth from Arêches meteorological station (1030 m high) at 4 km SW from Roselend. (c) Variations of lake water level through time and flow rates of tunnel dripping water measured in the HGZ and FZ.

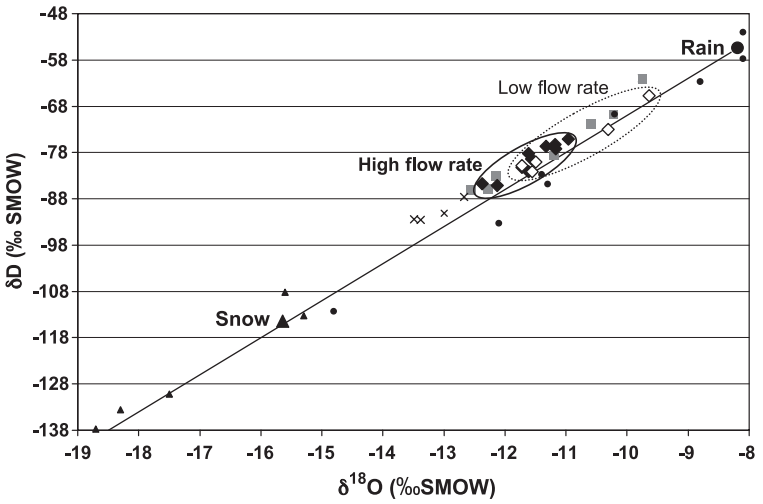

Fig. 3. δD vs. δ^{18}O compositions of waters. Tunnel dripping waters are divided into low flow rate (open diamonds) and high flow rate (closed diamonds) and overlap nearby groundwaters (shaded squares). Lake waters (crosses) are intermediate between local rain (large closed circle) and snow (large closed triangle). Compositions are shown for 1984 snow from Grimsel (triangles) and for 1999 undifferentiated precipitation from Thonon-les-Bains (circles) [7]. The δ-values of the latter decrease for September, October, April, November, February, December, January and March precipitation, respectively. Rain waters from May to August 1999 have higher δ-values not shown in the figure.

samples have been analyzed separately by capillary electrophoresis with uncertainties better than ±5%. To gain precision, part of the samples has also been analyzed by ion chromatography for anions and by ICP-OES for cations, with uncertainties of ±0.5% and 2%, respectively. No difference within uncertainties

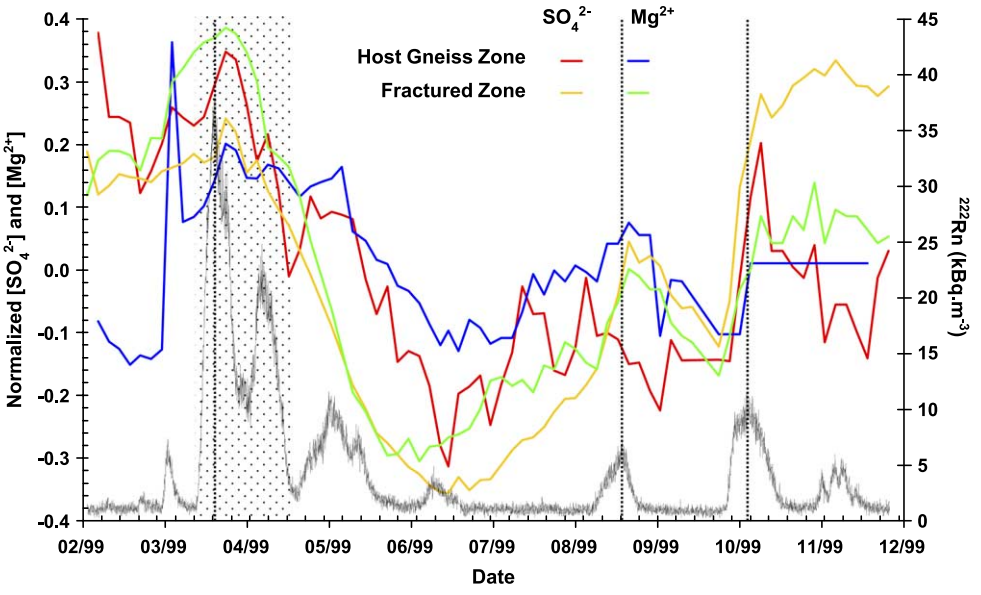

Fig. 4. SO_4^{2-} and Mg^{2+} normalized concentrations of dripping waters and radon activity in the tunnel atmosphere as a function of time. Transient increases in concentration appear simultaneously with radon bursts. The dashed lines indicate the same three main transient increases in concentrations as in Fig. 2; their exact position had been chosen to coincide with the peaks of radon bursts. The two large radon bursts observed from mid-March to mid-April could be viewed as a single broad episode indicated by the dotted area. Normalization is made so that each time series of ion concentration has a mean value of zero and the same amplitude; the data are not de-trended.

could be found between the two methods. The 1-year long monitoring of the dripping waters is presented in Fig. 2a for SO_4^{2-} and Mg^{2+}. These two conservative ions are not altered by calcium carbonate precipitation which has purity greater than 99%. Rainfall and snow depth, which quantify the input waters into the system, are presented in Fig. 2b. The lake level variations, which constitute the main mechanical forcing on the system [2] are presented in Fig. 2c. In addition, selected samples were analyzed for their D/H and $^{18}O/^{16}O$ ratios and are reported in the δ-notation in permil with reference to the SMOW standard. Isotopic compositions were measured on H_2 after U reduction of water [4], and on CO_2 after equilibration with water [5]. Results are presented in Fig. 3. Analytical precision was $\pm 1‰$ for hydrogen and $\pm 0.1‰$ for oxygen. Radon activity in the air of the tunnel was measured with a time step of 1 h by a Barasol™ counter [2] located at 57 m from the entrance (Fig. 1). Radon data are presented in Fig. 4.

4. Results

In the FZ, water drips at a rate of up to 2 orders of magnitude greater than in the HGZ, with minimum–maximum values of, respectively, 35–202 and 0.5–2.5 ml/h/m^2. This wide range in dripping water fluxes overlaps those measured all along the tunnel. Flow rates measured over more than 3 years at five places along the tunnel show synchronous seasonal variations with observed maximum in May and minimum in September. These high and low flow-rate periods correspond, respectively, to the meteorological wet and dry periods, with a delay of less than 3 months (Fig. 2). The annual volume of water dripping from the HGZ represents less than 1% of the annual precipitation per m^2. By contrast, the volume of water dripping in the FZ represents 44% of the annual precipitation per m^2. Depending on their distribution, fracture zones are therefore likely to constitute major recharge zones of the aquifers. Since the concentration variations measured in the two zones are nearly synchronous (Fig. 2a), this apparently similar water residence times for both HGZ and FZ indicates that fluid flow is mainly controlled by the fractures, taking into account the low porosity of the matrix. From the flow rates differing by a factor of 100, we infer that the equivalent permeability of the HGZ is about 100 times lower than that of the FZ.

The stable isotope compositions of input waters (rain and snow) and output waters (drip waters, water at nearby springs, and lake water) are presented in Fig. 3. All are meteoric waters. At mid Lat., the weighted annual oxygen isotope composition of precipitation varies with the mean annual surface air temperature [6]. Rain water taken from a puddle above the tunnel on September 20, 2001 represents a relatively warm period similar in composition to rain waters fallen in autumn at Thonon-les-Bains (80 km NNW from Roselend, altitude 385 m [7]). Rain waters from colder periods show lower δ-values. The coldest precipitation in Roselend occurs as snow and our sample comes from a 30-cm core, the depth of snow on January 27, 2000. Its composition is close to those of snow fallen in January and February 1984 at Grimsel (160 km NE from Roselend, altitude 1950 m [7]). Dripping waters sampled during relatively low flow-rate periods have higher δD and $\delta^{18}O$ values than those sampled during high flow-rate periods (Fig. 3). Interpreted in terms of variable input of local rain and melted snow waters, or variable precipitation temperatures, this is consistent with water residence times of less than 3 months. Indeed, the low flow-rate period (July–September) corresponds to limited infiltration of relatively warm rain water and no snow, whereas the high flow-rate periods (March–May) correspond to infiltration of colder rain and melted snow waters (Figs. 2b and 3).

The SO_4^{2-} and Mg^{2+} raw-data time series of waters dripping from the two sampling zones show systematic features (Fig. 2a). Mean concentrations are higher in the HGZ than in the FZ (1.94 meq/l for SO_4^{2-} and 1.35 meq/l for Mg^{2+} in the HGZ, 1.12 meq/l for SO_4^{2-} and 1.10 meq/l for Mg^{2+} in the FZ) and show smaller variations (0.33 meq/l for SO_4^{2-} and 0.50 meq/l for Mg^{2+} in the HGZ, 0.69 meq/l for SO_4^{2-} and 0.54 meq/l for Mg^{2+} in the FZ). The signals are almost synchronous (Fig. 4). They show a low frequency decrease in concentration (dilution) from the end of March to mid-June, as well as several high-frequency (4–16 days) increases in ion concentrations. Dilution coincides with melting of snow in rainy spring (Fig. 2a and b). The low frequency increase in concentration following spring dilution from mid-June to December indicates that pore waters are recharged in

ions by water–rock interactions. The residence time of water can be estimated from observations of the beginning of melting of snow to the beginning of dilution or, alternatively, from the end of melting of snow to the end of dilution. Values range from 25 to 60 days taking into account possible superimposed anomalies and possible effects of late snowfall in spring with little influence on dilution.

Three main transient increases in concentration, that occurred outside the spring dilution period, are readily identified, the end of March, in late August, and in early October (Fig. 2a). Especially after normalization (Fig. 4), additional transient increases in concentration could also be proposed but are less unambiguously supported by the data given the current resolution. Several transients might be observed between April and July, but the dilution period may have made them blurred. The normalized time series (Fig. 4) appear smoother for the FZ than for the HGZ, possibly due to the more direct flow occurring in the FZ. The transient increases in concentration cannot be related to rainfall events. An increase in concentrations due to rain or melting of snow events would require unlikely fast chemical reactions of these low salinity and cold waters with rock minerals, which is inconsistent since, in the same system, rain and melted snow transit are observed to cause dilution. These three main transient increases in concentration coincide, however, with peaks of radon levels in the tunnel (Fig. 4). These radon bursts are observed since 1995 with a rate of about 4 to 8 per year [8]. Although their generation mechanism is still poorly understood, they cannot be due to pressure variations only, and their repeated correlation with accelerated loading of the lake indicates a hydrogeological or a mechanical response of the rock matrix [2].

5. Discussion and conclusion

We propose a single in-situ mechanism where the ion concentration and radon changes are both generated locally. The fractured gneiss is a double porosity medium—matrix and fracture—with high fracture density in the FZ, and low fracture density in the HGZ. In both zones, fluid flow is controlled by the fractures. Advective fluid flow after rain or melted snow water infiltration occurs in the fractures, at low flow rates in the HGZ and at rates 100 times higher in the FZ with a similar apparent water residence time of 25 to 60 days which corresponds to the residence time of the fracture network. The matrix porosity contains water of longer residence time thus being more saline from longer interactions with minerals. In the FZ, predominantly made of quartz, high fluid flow rates in such sterile material produce low salinity dripping water, in contrast with the lower flow rates in the HGZ (Fig. 2). In each zone, the baseline ion concentrations reflect a steady-state dynamical equilibrium, involving low salinity, cold, rain and/or melted snow water input with kinetically limited chemical interactions along the flow path, and limited input of more saline water stored in the matrix porosity. Such limited connections between the matrix porosity and the fractures are probably controlled by diffusion.

However, if advective transfer of water from the matrix to the fractures is triggered by a hydrogeological or mechanical process such as increases in pore pressure or changes in the fracture network geometry, transient concentration increases could appear in this system. In such case, either the pressure differential or the conductance between the matrix and the fractures is larger. Similarly, release of radon present at high concentrations in the matrix porosity [9] could be triggered by pressure changes or crack reorganization and produce the radon anomalies observed in the tunnel after transport in the fractures. In June, we observe a low-intensity radon burst with apparently no associated chemical transient (Fig. 4). This could be explained, at the end of the dilution period and after four radon bursts in 2.5 months, including the three largest ones, by the matrix porosity being exhausted and unable to provide sufficient matter for anomalies.

The load of the lake is expected to induce extensional strain in the matrix, thus, it is likely that the conductance between the matrix and the fractures is increased, expectedly by changes in the fracture network geometry or opening of pre-existing fracture. Fracturing of the rock mass is not likely as the same load has been repeated on every annual cycle, and fractures are not expected to heal in this environment. The detailed mechanism responsible for the March as opposed to the September events could be different as the loading rates and lake levels are different for each.

Other differences in the response of the FZ compared with the HGZ, or SO_4^{2-} compared with Mg^{2+}, could be attributed to complex fracture–matrix relationships, heterogeneous mineralogy of the rocks, or variable water content if the rocks above the tunnel are in the vadose zone. From the mass balance calculation, with the chemistry of the matrix water estimated from that of the HGZ, the volume of water discharged from the host rock to the FZ represents up to 40% of the amount of water in the FZ. However, we have no constraints on the lower limit since the HGZ fluid is only partly composed of matrix water as indicated by the transient anomalies also observed for the HGZ. Unfortunately, a monitoring of the dripping water flow rates was not available at the time of the experiment. This experiment points out the need for simultaneous monitoring of both flow rates and ion concentrations [3].

Our experimental results therefore suggest that during the hydrogeological or mechanical perturbation of fractured rocks, transient water and gas discharges occur from matrix pores to the fractures. This mechanism generalizes a preliminary work from Gascoyne and Thomas [10] and may be of interest for the understanding of the mechanisms leading to earthquake precursors. Indeed, in our system, one important forcing is the mechanical effect of the variations of lake level [2]. However, a lot remains to be done to link the mechanics to the observed hydrochemical anomalies. In particular, the complex problem of estimating in-situ stress, rock strength, and possible rock failure is beyond the scope of this paper. As a preliminary result, order of magnitude estimation of the associated strain can be done as follows. On a semi-infinite space locally deformed by applied forces, the stress variation σ at the tunnel is of the order of $F/\pi r^2$ [11] where F is the weight of water (180×10^9 kg for the full range of level variations) and r is the distance between the tunnel and the center of gravity of the lake (ca. 1000 m), which amounts to about 6 bars. The corresponding deformation is given by $\theta=\sigma/E$, where E is the Young modulus (8×10^{10} Pa [12] for the Roselend site) and amounts to about 7 μrad (or similarly a few microstrains), which is in good agreement with the amplitude of tilt variation measured in the tunnel [2]. This deformation is of the same order of magnitude as the expected preseismic strain in the epicentral zone (10^{-5}, [13]). If the anomalies observed in Roselend are due to mechanical variations, then the same mechanism could account for anomalies observed before earthquakes, notwithstanding the time scales. Groundwater and gas anomalies have been reported with many earthquakes, among which sulfate and radon are particularly cited [14–16], even though they are not usually related to a single cause as here. The main tentative explanation for geochemical anomalies is aquifer mixing [17–19] although the identification of the aquifers supposed to mix their waters remains questionable [20]. Furthermore, Igarashi et al. [21] and Sano et al. [22] showed from their studies in the Kobe area, that the two existing aquifers are not likely to have mixed their water and called for a role of microfractures in the generation of geochemical anomalies. The presented mechanism appears as a relevant alternative to the widely called aquifer mixing and our methodology should therefore be relevant for current and future long-term observatories in active tectonic environments.

Acknowledgements

We thank Simon M.F. Sheppard for the fruitful discussions and for the stable isotope compositions of the waters, Arnaud Martin-Garin for an early work on the data; Jean Aupiais for capillary electrophoresis analyses, Martine Musso-Lanson for the assistance in the field, ion chromatography and ICP-OES analyses. Thanks go to EDF for the lake level data, and to the IAEA GNIP stations and laboratories. This manuscript benefited from the constructive remarks of Evelyn Roeloffs, and from the reviews of Jean-Claude Baubron and Ghislain de Marsily.

References

[1] A.L. Flint, L.E. Flint, G.S. Bodvarsson, M. Kwicklis, J. Fabryka-Martin, Evolution of the conceptual model of unsaturated zone hydrology at Yucca Mountain, Nevada, J. Hydrol. 247 (2001) 1–30.

[2] M. Trique, P. Richon, F. Perrier, J.-P. Avouac, J.-C. Sabroux, Radon emanation and electric potential variations associated with transient deformation near reservoir lakes, Nature 399 (1999) 137–141.

[3] A.-S. Provost, P. Richon, E. Pili, F. Perrier, S. Bureau, Fractured porous media under influence: the Roselend Experiment, EOS Trans., AGU 85 (12) (2004) 113.

[4] J. Bigeleisen, M.L. Perlman, H.C. Prosser, Conversion of hydrogenic materials to hydrogen for isotopic analysis, Anal. Chem. 24 (1952) 1356–1357.
[5] R.A. Socki, H.R. Karlsson, E.K. Gibson Jr., Extraction technique for the determination of oxygen-18 in water using pre-evacuated glass vials, Anal. Chem. 64 (1992) 829–831.
[6] W. Dansgaard, Stable isotopes in precipitation, Tellus 16 (1964) 436–468.
[7] IAEA/WMO, Global Network for Isotopes in Precipitation. The GNIP Database, 2002.
[8] P. Richon, F. Perrier, J.-C. Sabroux, M. Trique, C. Ferry, V. Voisin, E. Pili, Spatial and time variations of radon-222 concentration in the atmosphere of a dead-end horizontal tunnel, J. Env. Rad., in press.
[9] W.W. Nazaroff, Radon transport from soil to air, Rev. Geophys. 30 (1992) 137–160.
[10] M. Gascoyne, D.A. Thomas, Impact of blasting on groundwater composition in a fracture in Canada's Underground Research Laboratory, J. Geophys. Res. 102 (B1) (1997) 573–584.
[11] J.C. Jaeger, N.G.W. Cook, Fundamentals of Rock Mechanics, Methuen and Company, London, 1969, 513 pp.
[12] Électricité de France, Note de synthèse géologique et technique, Barrage de Roselend, Fondation de l'Ouvrage (in French) p. 12, Aix-en-Provence, 1962.
[13] P. Bernard, Plausibility of long distance electrotelluric precursors to earthquakes, J. Geophys. Res. 97 (1992) 17,531–17,546.
[14] U. Tsunogai, H. Wakita, Precursory chemical changes in ground water: Kobe earthquake, Japan, Science 269 (1995) 61–63.
[15] F. Bella, P.F. Biagi, M. Caputo, E. Cozzi, G. Della Monica, A. Ermini, E.I. Gordeez, Y.M. Khatkevitch, G. Martinelli, W. Plastino, R. Scandone, V. Sgrigna, D. Zilpimiani, Hydrogeochemical anomalies in Kamchatka (Russia), Phys. Chem. Earth 23 (9–10) (1998) 921–925.
[16] S. Nishizawa, G. Igarashi, Y. Sano, Radon, Cl^- and SO_4^{2-} anomalies in hot spring water associated with the 1995 earthquake swarm off the east coast of the Izu Peninsula, central Japan, Appl. Geochem. 13 (1998) 89–94.
[17] C.-Y. King, W.C. Evans, T. Presser, R.H. Husk, Anomalous chemical changes in well waters and possible relations to earthquakes, Geophys. Res. Lett. 8 (5) (1981) 425–428.
[18] D. Thomas, Geochemical precursors to seismic activity, Pure Appl. Geophys. 126 (2–4) (1988) 241–266.
[19] J.P. Toutain, M. Munoz, F. Poitrasson, A.C. Lienard, Springwater chloride ion anomaly prior to a Ml=5.2 Pyrenean earthquake, Earth Planet. Sci. Lett. 149 (1997) 113–119.
[20] F. Poitrasson, S.H. Dundas, J.P. Toutain, M. Munoz, A. Rigo, Earthquake-related elemental and isotopic lead anomaly in a springwater, Earth Planet. Sci. Lett. 169 (1999) 269–276.
[21] G. Igarashi, S. Saeki, K. Takahata, K. Sumikawa, S. Tasaka, Y. Sasaki, M. Takahashi, Y. Sano, Ground-water radon anomaly before the Kobe earthquake in Japan, Science 269 (1995) 60–61.
[22] Y. Sano, N. Takahata, G. Igarashi, N. Koizumi, N. Sturchio, Helium degassing related to the Kobe earthquake, Chem. Geol. 150 (1998) 171–179.